The 2004 IEEE International Conference on Speech, Acoustics, and Signal Processing (ICASSP 2004)
Montreal, May 17–21, 2004, http://www.icassp2004.com/

PING-PONG SAMPLE TIMES ON A LINEAR ARRAY HALVE THE NYQUIST RATE

Jeffrey O. Coleman
http://alum.mit.edu/www/jeffc

Naval Research Laboratory (http://www.nrl.navy.mil/)
Radar Division, Signal Processing Theory & Methods Section

***Abstract*— Staggering the sample times for alternate elements of a linear antenna array is shown to halve the usual Nyquist sample-rate bound of twice the one-sided signal bandwidth while preserving alias-free mapping between spectral components and plane waves in the far field. The approach can be used on transmit or receive and with lowpass or bandpass sampling, and it can involve analog up- or down-conversion between data conversion and the array. The usual element-spacing bound of half a wavelength at the upper RF band edge is replaced with a quarter-wavelength bound at the center of the Nyquist sampling band referred to RF, a reduction only for bandpass sampling.**

1 INTRODUCTION

Sampled-data systems operating directly on RF and IF signals are proposed with increasing frequency and often with separate, per-channel processing for each element of a phased array. Generally however, sampling in time and the sampling in space implicit in a linear array are considered separately, and the two sampling processes are therefore subject to separate Nyquist limits. In wideband systems, however, array elements spaced at the $\lambda/2$ spatial Nyquist limit at the upper RF band edge are spaced considerably closer, in terms of $\lambda = c/|f|$, at the lower band edge. The alternative presented here is to design the temporal and spatial sampling jointly using a minimum of lattice theory—a few pages of Conway and Sloane's lattice bible [1] are involved—to avoid this wasteful spatial oversampling. A system results in which sample timing differs by $180°$ for even- and odd-numbered array elements. Remarkably, the required temporal sample rate is halved with the element density increased by less than a factor of two for bandpass (temporal) sampling and unchanged for lowpass (temporal) sampling. The lower sample rate simplifies array-beam realization, and array-pattern design [2] is straightforward using modern optimization techniques.

The remaining two sections present the idea in detail and in summary respectively, and the figures and captions alone form a reasonably self-contained intermediate-level overview.

This work was supported by the Office of Naval Research, the Defense Advanced Research Projects Agency, and the base-funding program at the Naval Research Laboratory,

2 SAMPLES ON A LATTICE AND SPECTRAL REPLICATION

The sample-location lattice. Finitely many signal samples —from power-up to power-down is a finite interval—applied to or sampled from finitely many array elements can be represented by a complex Borel measure $\underline{y}$ with support on some finite subset of $\mathbb{R}^4$, each 4D point $\mathbf{t}$ of which represents a pair $(\mathbf{x}, ct)$ of spacetime coordinates. Scaling time by c gives all elements of $\mathbf{t}$ length units. The usual 1D assumption of samples at times $T\mathbb{Z}$ for some sample interval T has as its parallel in 4D spacetime the assumption that signal measure $\underline{y}$ has support contained in some *sample-location lattice* $\mathbf{T}\mathbb{Z}^M$ defined by a $4 \times M$ generating matrix $\mathbf{T}$, in DSP a *sample-interval matrix*, with linearly independent columns. The elements of $\mathbf{T}\mathbb{Z}^M$ comprise all possible integer combinations of those columns, the lattice basis vectors. When $\underline{y}$ has this structure it can be expressed in terms of 4D impulses as

$$d\underline{y} = \sum_{\mathbf{n} \in \mathbb{Z}^M} y_{\mathbf{n}}\, \delta(\mathbf{t} - \mathbf{T}\mathbf{n})\, d\mathbf{t}, \tag{1}$$

where only a finite number of *samples* $y_{\mathbf{n}}$ are nonzero.

The number M of lattice basis vectors, the dimension of the lattice, is important here. The $M = 1$ case with $\mathbf{T} = (0, 0, 0, cT)^T$ corresponds to a conventional 1D sampled signal on a zero-dimensional "array" comprising a single element at the origin. The $M = 2$ case, the focus of this paper, corresponds to a linear array. The special case with

$$\mathbf{T} = \begin{pmatrix} d\widehat{u} & 0 \\ 0 & cT \end{pmatrix} \tag{2}$$

is illustrated in Fig. 1 and represents a conventional 1D sampled signal on each element of a linear array aligned with dimensionless 3D unit vector $\widehat{u}$. A planar array with elements located on a lattice has $M = 3$, and the uncommon $M = 4$ case represents an array on a 3D lattice. This paper does not deal with offset lattices but assumes a sample at the 4D spacetime origin. The extension to offset lattices is straightforward but tedious. Actual design of sample-location lattices for the $M = 3$ and $M = 4$ cases is beyond the scope of this paper, but the principles mirror those presented here.

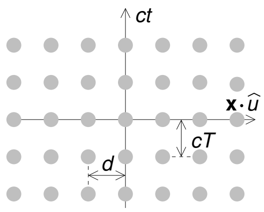

Figure 1: Array elements spaced at interval d along direction $\widehat{u}$ and driven or sampled synchronously at interval T have spacetime samples on this rectangular sample-location lattice. Both axes have length units.

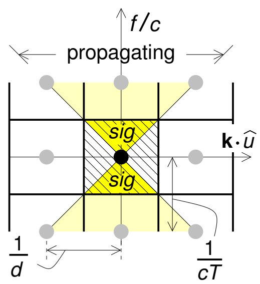

Figure 2: Fourier transforming the Fig. 1 samples tiles the plane with translations of the spectrum in the first Nyquist zone (hatched) by offsets in this spectral-replication lattice, the dual of the Fig. 1 sample-location lattice. If $d \le \frac{\lambda}{2}$ in signal band $|fT| \le \frac{1}{2}$, then propagating Fourier components, with $\|\mathbf{k}\| < \frac{|f|}{c}$, are in this Nyquist zone.

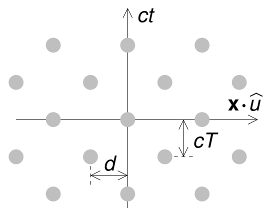

Figure 3: The sample-location lattice of Fig. 1 is modified here by omitting half the samples, in checkerboard fashion. It is otherwise unchanged.

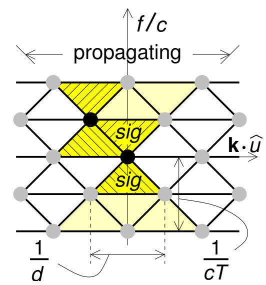

Figure 4: Propagating $(\mathbf{k}, f/c)$ pairs with $|fT| < \frac{1}{2}$ form a butterfly-shaped signal region ("sig") that becomes the first Nyquist zone and tiles the plane using offsets from this spectral-replication lattice, the dual of the Fig. 3 sample-location lattice. One offset spectral replica is shown. Halving the sample density in Fig. 3 has doubled the lattice density here and eliminated the unused half of the first Nyquist zone in Fig. 2.

Table 1: Comparison of lowpass-sampling approaches.	*rectangular sampling*	*ping-pong sampling*
sample-location lattice	Fig. 1	Fig. 3
spectral-replication lattice	Fig. 2	Fig. 4
element spacing, top of band	$\lambda/2$	$\lambda/2$
per-element sample rate f_s	T^{-1}	$(2T)^{-1}$
top of signal band	$f_s/2$	f_s

The spectral-replication lattice. In 1D DSP a signal with samples in $T\mathbb{Z}$ has a Fourier transform that has period T^{-1} and that therefore is invariant to translations by elements of $T^{-1}\mathbb{Z}$. Conversely, a signal with a transform invariant to translations from $T^{-1}\mathbb{Z}$ certainly has temporal support in $T\mathbb{Z}$, but that support might lie entirely in some subset $NT\mathbb{Z}$. Its spectrum would be invariant to translations from $(NT)^{-1}\mathbb{Z}$ as well as from subset $T^{-1}\mathbb{Z}$. Care with the analogous 4D point will be required.

By (1) the Fourier transform of signal measure $\underline{y}$ is

$$\mathrm{Y}(\mathbf{f}) = \int \mathrm{e}^{-\mathrm{j}2\pi\mathbf{f}^T\mathbf{t}}\, d\underline{y}(\mathbf{t}) = \sum_{\mathbf{n}\in\mathbb{Z}^M} y_{\mathbf{n}}\, \mathrm{e}^{-\mathrm{j}2\pi\mathbf{f}^T\mathbf{T}\mathbf{n}}\,.$$

Here $\mathbf{f}$ represents 4D frequency coordinates $(\mathbf{k}, f/c)$, where 3D vector $\mathbf{k}$ is a the negative of the wavenumber and where normalizing frequency f gives all elements of $\mathbf{f}$ inverse length units. The next few paragraphs are more general, however, as time $\mathbf{t}$, frequency $\mathbf{f}$, and the various lattice basis vectors can have identical but arbitrary dimensionality.

To what translations is $\mathrm{Y}(\mathbf{f})$ invariant? Suppose sample-interval matrix $\mathbf{T}$ has M linearly independent columns as before, and suppose also that the M columns of some matrix $\mathbf{A}$ are basis vectors for a lattice of frequency points. Translation of $\mathrm{Y}(\mathbf{f})$ by a point from that lattice can be written

$$\mathrm{Y}(\mathbf{f}+\mathbf{A}\mathbf{k}) = \sum_{\mathbf{n}\in\mathbb{Z}^M} y_{\mathbf{n}}\, \mathrm{e}^{-\mathrm{j}2\pi(\mathbf{f}^T\mathbf{T}\mathbf{n}+\mathbf{k}^T\mathbf{A}^T\mathbf{T}\mathbf{n})},$$

where $\mathbf{k} \in \mathbb{Z}^M$ is arbitrary. Therefore, $\mathrm{Y}(\mathbf{f}+\mathbf{A}\mathbf{k}) = \mathrm{Y}(\mathbf{f})$ for arbitrary $\mathbf{k} \in \mathbb{Z}^M$ and sample sequence $y_{\mathbf{n}}$ if and only if $M \times M$ matrix $\mathbf{Z} \triangleq \mathbf{A}^T\mathbf{T}$ has only integer elements.

This condition makes the spectrum invariant to translations from lattice $\mathbf{A}\mathbb{Z}^M$, but might $\mathbf{A}\mathbb{Z}^M$ be a sublattice of some more-dense lattice for which translation invariance also holds? Suppose $\mathbf{Z}$ is indeed an integer matrix, and assume $\mathbf{A}$ is such that $\mathbf{Z} = \mathbf{A}^T\mathbf{T}$ is invertible as well. Define an M column matrix $\Delta\mathbf{f}$ by $\Delta\mathbf{f}^T = \mathbf{Z}^{-1}\mathbf{A}^T$ so that $\mathbf{A} = \Delta\mathbf{f}\,\mathbf{Z}^T$. Certainly $\mathbf{Z}^T\mathbb{Z}^M \subset \mathbb{Z}^M$, as $\mathbf{Z}$ is an integer matrix, so lattice

$$\mathbf{A}\mathbb{Z}^M = \Delta\mathbf{f}\,\mathbf{Z}^T\mathbb{Z}^M \subset \Delta\mathbf{f}\,\mathbb{Z}^M. \tag{3}$$

But

$$\Delta\mathbf{f}^T\mathbf{T} = \mathbf{Z}^{-1}\mathbf{A}^T\mathbf{T} = \mathbf{Z}^{-1}\mathbf{Z} = \mathbf{I}, \tag{4}$$

an integer matrix also, so in addition to $\mathrm{Y}(\mathbf{f}+\mathbf{A}\mathbf{k}) = \mathrm{Y}(\mathbf{f})$,

$$\mathrm{Y}(\mathbf{f}+\Delta\mathbf{f}\,\mathbf{k}) = \mathrm{Y}(\mathbf{f}) \tag{5}$$

for arbitrary $\mathbf{k} \in \mathbb{Z}^M$. As lattice $\mathbf{A}\mathbb{Z}^M$ is a sublattice of $\Delta\mathbf{f}\,\mathbb{Z}^M$ by (3), frequency-domain periodicity condition (5) includes the earlier one. *Spectral-replication lattice* $\Delta\mathbf{f}\,\mathbb{Z}^M$ is the *dual* of sample-location lattice $\mathbf{T}\mathbb{Z}^M$, because generating matrix $\Delta\mathbf{f}$, the *spectral-period matrix,* is defined by $\Delta\mathbf{f}^T\mathbf{T} = \mathbf{I}$ in (4) and so is the pseudoinverse of sample-interval matrix $\mathbf{T}$. The original lattice generating matrix $\mathbf{A}$ is unnecessary, and all parallels the usual 1D case with astonishing elegance.

Conventional sample placement. The conventional data-converter interface to a linear array uses the spacetime samples shown in Fig. 1 and is characterized by the sample-interval matrix $\mathbf{T}$ of (2). The spectral-period matrix becomes

$$\Delta\mathbf{f} = \begin{pmatrix} \frac{1}{d}\widehat{u} & 0 \\ 0 & \frac{1}{cT} \end{pmatrix},$$

and results in the spectral-replication lattice shown in Fig. 2.

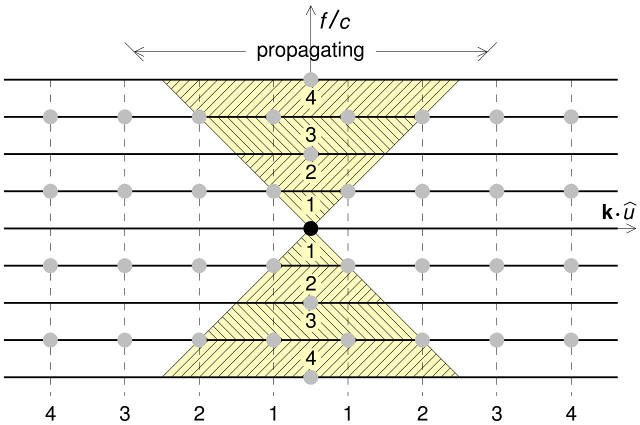

Figure 5: Nyquist zone m (hatched) for $m = 1, ..., 4$ splits into two nontouching regions for $m > 1$ and tiles the plane with offsets from a checkerboard spectral-replication lattice that includes the the central column of dots and the two columns of dots labeled m. Nyquist zone 1 represents lowpass sampling and was discussed in Figs. 1–4 and Table 1. The other Nyquist zones represent bandpass sampling.

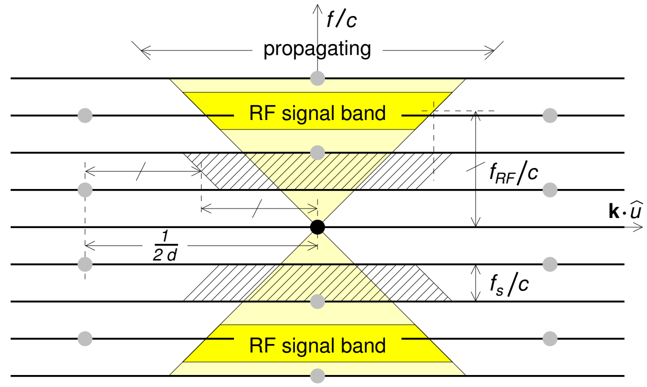

Figure 6: Frequency conversion can be used between the elements and bandpass-sampling data conversion. The Nyquist zone (hatched) has its vertical extent set at IF to effect bandpass sampling but has its width determined at RF—the band is arbitrary—to match the Helmholz cone. Element spacing becomes $\lambda/4$ at f_{RF}, the center of the Nyquist band RF referred to RF. The per-element sample rate is $f_s = \frac{1}{2T}$.

Nyquist zones. The hatched rectangle at the center in Fig. 2 can be taken as one period of the transform. The plane is precisely tiled by offsetting this period region by the points of the spectral-replication lattice, and the transform behaves identically on each tile. In lattice theory a single tile is a *fundamental volume* of the lattice [1]. In DSP it is a *Nyquist zone*. The shape of the fundamental volume or Nyquist zone is not unique, as Dutch artist M.C. Escher so elegantly demonstrated by tiling planes with interlacing birds and fish (typically each of his fundamental volumes comprised two or more animals), and a Nyquist zone need not contain the origin and need not even be simply connected. Let us designate the hatched region in Fig. 2 as the first of many standard Nyquist zones. If a signal on continuous 4D variable $\mathbf{t}$ contains spectral components only inside a single Nyquist zone, it can be represented in sampled form exactly, without aliasing.

Propagation and the Helmholz cone. A receive array samples far-field plane waves in time and space, and a transmit array creates far-field plane waves from its input samples. (We "factor out" the element pattern.) The Fourier integral

$$\int \mathbf{E}(\mathbf{f})\, \mathrm{e}^{\mathrm{j}2\pi \mathbf{f}^T \mathbf{t}}\, d\mathbf{f},$$

in 4D describes the electric field as a plane-wave sum when complex 3D vector $\mathbf{E}(\mathbf{f})$ is DC-free, orthogonal to wavenumber $-\mathbf{k}$, and supported only in $\{(\mathbf{k}, f/c) : \|\mathbf{k}\| \leq |f|/c\}$, the *Helmholz cone* [3] that relates temporal frequency f to physical wavelength $1/\|\mathbf{k}\|$ for propagating plane wave $\mathrm{e}^{\mathrm{j}2\pi \mathbf{f}^T \mathbf{t}} = \mathrm{e}^{\mathrm{j}2\pi(ft + \mathbf{k}\cdot\mathbf{x})}$. The Helmholz cone is the area within 45° of the vertical axis in Fig. 2, where the assuming $\lambda/2$ array-element spacing at the upper band edge sets $d = cT$. A receive array's far-field input has no components outside the Helmholz cone, and a transmit array cannot create such components. Physics puts a 4D "Helmholz-pass filter" between the array and the far field, so points outside the Helmholz cone are of no use in an array transmitter or receiver's Nyquist zone. Half of the first Nyquist zone in Fig. 2 is outside the Helmholz cone and useless.

A butterfly in the Helmholz cone: ping-pong sample times. The shape of the first Nyquist zone will be better matched to the Helmholz cone if the sample-location lattice of Fig. 1 is replaced with the half-density sublattice shown in Fig. 3. The sample-interval and spectral-period matrices

$$\mathbf{T} = \begin{pmatrix} d\widehat{u} & 0 \\ d & 2cT \end{pmatrix} \qquad \Delta\mathbf{f} = \begin{pmatrix} \frac{1}{d}\widehat{u} & \frac{-1}{2cT} \\ 0 & \frac{1}{2cT} \end{pmatrix}$$

result in $\Delta\mathbf{f}^T\mathbf{T} = \mathbf{I}$ and, again along with $d = cT$, replace the Fig. 2 spectral-replication lattice with the Fig. 4 double-density superlattice. Back and forth, "ping-pong" sample times alternating between even- and odd numbered array elements are created by a checkerboard sample-location lattice in spacetime. A checkerboard spectral-replication lattice results and nicely tiles the plane with translations of a Nyquist zone that is the Helmholz cone truncated to a butterfly.

First Nyquist zone: sample-rate requirement halved. Table 1 compares the two approaches. Given a signal band they require identical element spacing, but ping-pong sample times halve the per-element sample rate f_s. The usual 3 dB white-noise advantage of 2 × oversampling is lost, as digital filtering can no longer remove quantization noise and receiver front-end noise that falls outside the Helmholz cone.

Bandpass sampling: other Nyquist zones. Figure 5 shows the first Nyquist zone and three alternative Nyquist zones in the Helmholz cone for ping-pong sampling times. A signal band in the first Nyquist zone is *lowpass sampling* because f there approaches DC arbitrarily closely. Using a Nyquist zone bounded away from $f = 0$ as the signal band yields *bandpass sampling*. Tiling the plane with the wider Nyquist zones requires stretching the spectral-replication lattice horizontally by decreasing element spacing d. (The relationship between d and lattice points remains as in Fig. 4.)

Frequency conversion. Analog frequency conversion in either direction can be used in either a transmit or receive system as illustrated in Fig. 6. The Nyquist-zone idea applies at IF, where data conversion is done, so the IF band must lie between successive integral multiples of per-channel sample rate $f_s = \frac{1}{2T}$. After the width of the Nyquist zone is fixed at RF to exactly span the Helmholz cone, the horizontal scale of the spectral-replication lattice is set, by fixing element spacing d, for correct tiling of the plane. Ultimately, element spacing $d = \lambda/4$ at the center f_{RF} of the RF band. These design rules apply to the ping-pong configurations of Figs. 4 and 5 if the RF and IF bands are taken as identical.

Adding $\Delta\Sigma$ noise bands. The Nyquist zone in any $\Delta\Sigma$ system must include significant spectral space for noise. In spacetime $\Delta\Sigma$ D/A conversion [4] that noise is then removed by analog filtering and the array's Helmholtz-pass filtering. Decreasing d to spread the spectral-replication lattice horizontally as in Fig. 7 can create an arbitrary-width noise band.

Guard bands for beam design. The bands labeled "noise" in Fig. 7 can be used as guard bands instead when a little extra Nyquist-zone width is desired to permit a pattern beam at one (spatial) edge of the signal band from unduly influencing the sidelobes at the other end through periodic replication.

3 SUMMARY

When a transmitter or receiver uses an array of linearly spaced antenna elements and uses sampled-data signal paths for individual elements, only even-numbered samples are actually needed for even-numbered array elements, and only odd-numbered samples are needed for odd-numbered array elements. This ping-pong alternation of the sample instants for even- and odd-numbered array elements lowers the required per-channel sample rate by half.

The ping-pong Nyquist rule is simple. If f_s denotes the per-element sample rate, the mth Nyquist band in the part of the system, RF or IF, where data conversion to or from analog takes place extends from $(m-1)f_s$ to mf_s, with integer $m \geq 1$. If f_{RF} denotes the RF frequency corresponding via any analog frequency conversion used to the center of

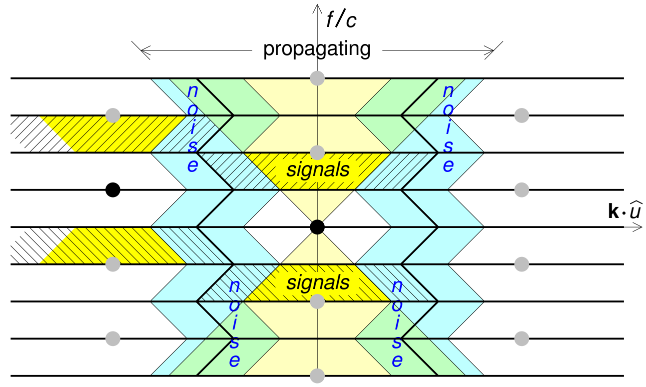

Figure 7: Reduced element spacing d here extends the second Nyquist zone beyond the Helmholz cone, creating a noise band for use by a spacetime $\Delta\Sigma$ modulator. One spectral copy from the tiling of the plane is shown.

this Nyquist band, the array-element spacing must be at least $\lambda_{RF}/4$, where $\lambda_{RF} = c/f_{RF}$. When $m = 1$, the lowpass-sampling case, no element-density penalty is incurred as this is just the usual half-wavelength element spacing at the upper sampling-band edge mf_s after referral to RF. In the $m > 1$ bandpass-sampling cases the cost in increased element density is less than a factor of two.

Fundamentally, the sample-rate savings accrues by elimation of a redundancy implicit in the shape of the Nyquist regions associated with conventional sample timing. Conventional systems are needlessly capable of representing spectral components that do not correspond to propagating plane waves because they do not satisfy the $\|\mathbf{k}\| \leq |f|/c$ Helmholz relation between wavenumber $-\mathbf{k}$ and temporal frequency f. The ping-pong sample times allow the Nyquist region repliced spectrally to be chosen to include only components satisfying the Helmholz relation, thus eliminating the redundancy.

REFERENCES

[1] J. H. Conway and N. J. A. Sloane, *Sphere Packings, Lattice and Groups*, Springer-Verlag (http://www.springer.com), 2nd ed., 1988.

[2] D. P. Scholnik and J. O. Coleman, "Superdirectivity and SNR constraints in wideband array-pattern design," in *IEEE Int'l Radar Conference* (Atlanta), May 2001.

[3] C. A. Balanis, *Antenna Theory*, John Wiley & Sons, Inc., (http://www.wiley.com), 1982.

[4] D. P. Scholnik and J. O. Coleman, "Space-time vector delta-sigma modulation," in *IEEE Int'l Conf. on Circuits and Systems* (Phoenix, AZ), May 26–29, 2002.